

Sample preparation

To make graphene membranes, we started with graphene flakes prepared on top of an oxidized silicon wafer (300 nm of SiO₂) by micromechanical cleavage, as described previously [1,9]. Monolayer flakes were identified by optical microscopy from a subtle shift in colour [1,9] as compared to the empty surface (Fig. S1A) and, if in doubt, this was double-checked by atomic force microscopy [1,9]. A metal grid (3 nm Cr and 100 nm Au) was then deposited on top of a chosen flake by using electron-beam lithography. After that, the substrate was cleaved so that its edge was within 50 μm from the chosen flake (Fig. S1B). These samples were put in 15% tetramethylammonium hydroxide at 60 °C for several hours, which etched away the bulk Si, undercutting the grid. The etching was monitored through an optical microscope and stopped after a sufficient part of the grid became overhanging (Fig. S1C). The remaining SiO₂ layer was removed during 5 minutes in 6% buffered hydrofluoric acid. The samples were then transferred into water, isopropanol, acetone and, finally, liquid carbon dioxide for critical point drying. Fig. S1C,D show the resulting scaffold with the flakes attached underneath it.

Numerical simulations

To estimate the spatial size of the microscopic crumpling, we have performed simulations of the electron diffraction patterns that are expected for non-flat graphene sheets in the partially coherent illumination of our TEM. To this end, we took a flat graphene sheet (Fig. S2A) and added to this out-of-plane (*z*) displacements with single-frequency components given by $z(x,y)=A\sin(k_x x+k_y y+B)$ where *A*, *B*, *k_x*, *k_y* were random parameters. A single-frequency component is shown in Fig. S2B. A large number of such sinusoidal waves were superimposed to obtain a randomly curved sheet, as shown in Fig. S2C. The random parameters were distributed so that desired average for out-of-plane deformation *h* and for a lateral ripple size *L* were obtained. For each tilt angle, the projected atomic potentials were then calculated by using a 10 nm area of the sheet (the lat-

ter size corresponds to the coherence length of electrons in our experiments). After this, we calculated the Fourier transform of the projected potentials, which yields diffraction patterns from each coherently illuminated area of 10 nm in size. Because experimentally we worked with the smallest possible but still relatively large beam (250 nm in diameter), we calculated diffraction patterns from many coherently illuminated units and added up their intensities.

The described simulation at different tilt angles were carried out for various sizes and heights of the ripples. In all the cases, the average waviness was fixed at 5° (as measured experimentally), which corresponds to ratio $L/h \approx 10$ between ripples' lateral size *L* and their height *h*. Figures S3 to S5 show examples of the resulting simulations of diffraction patterns for a tilt angle of 26°, which mimics the experimental situation in Fig. 2E of the main paper. If ripples' size is notably smaller than the electron coherence length, the simulated diffraction pattern displays sharp peaks (Fig. S3), in clear disagreement with our experimental observations. In the opposite limit of ripples larger than the coherence length (Fig. S5), diffraction spots become representative of the actual local bending of a graphene sheet. This contradicts to our experiment, where we observe diffraction peaks with a smooth Gaussian shape, independently of the spot position and using different samples. This indicates that in our case the average ripple size should be of the order of the electron coherence length. In this case, the simulated peak broadening (Fig. S4) closely resembles our experimental data in Fig. 2 and 3. Further comparison between the simulations and experiment infers ripples' lateral size of 5 to 10 nm. However, because of experimental uncertainty in the actual coherence length, which may be a factor of 2 larger or smaller than the value of 10 nm used in our simulations, we make a prudent estimate for the typical lateral size of crumpling as between 2 and 20 nm.

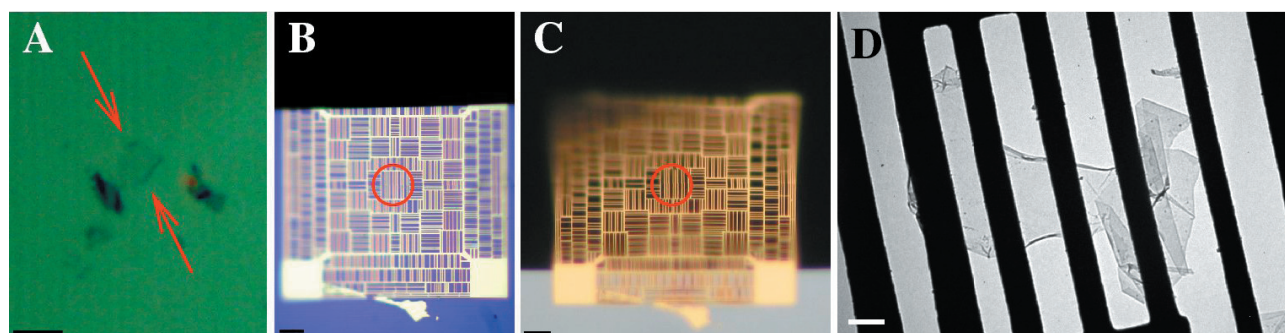


Figure S1: Preparation of suspended graphene membranes. A, Optical micrograph of a single-layer graphene sheet (arrows) on an oxidized Si substrate, which is surrounded by a few thicker flakes. B, Metal grid deposited on top of the graphene sheet. C, Part of the substrate is removed by chemical etching so that the metal

grid reaches over the substrate edge. The graphene sheet (marked by red circles in B and C) remains attached to the metal scaffold. D, Bright-field TEM image of a suspended graphene membrane. Scale bars: 5 μm (A), 10 μm (B,C) and 500 nm (D).

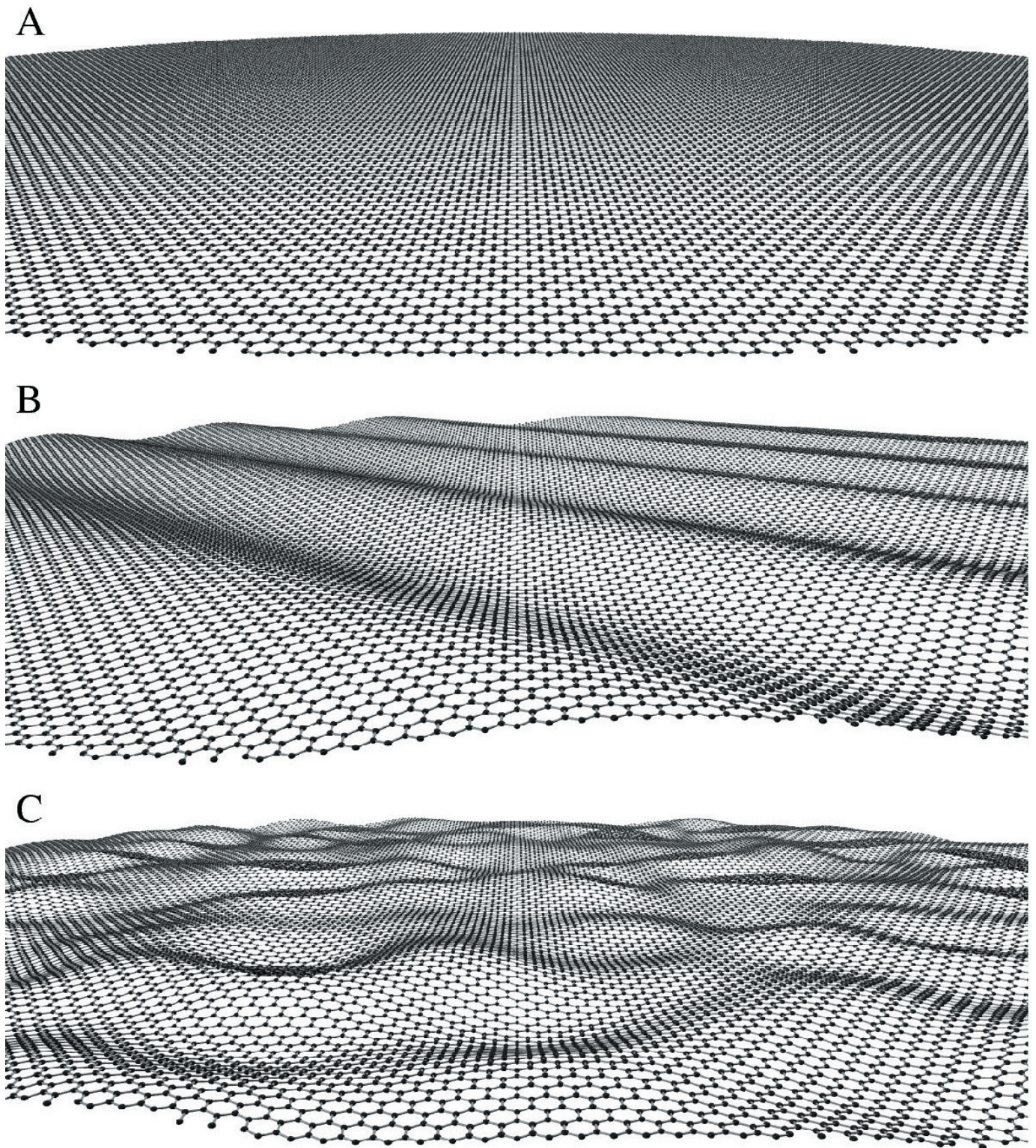
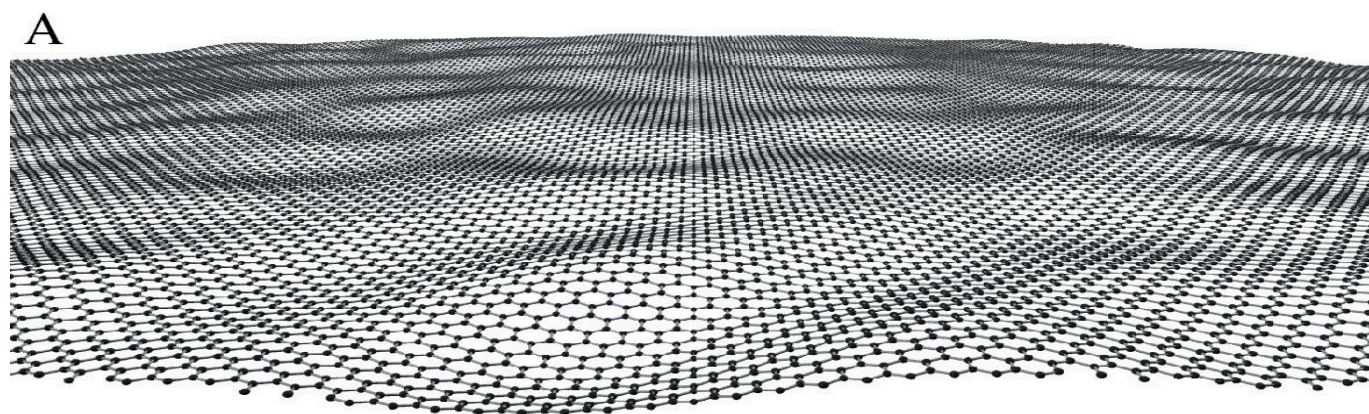


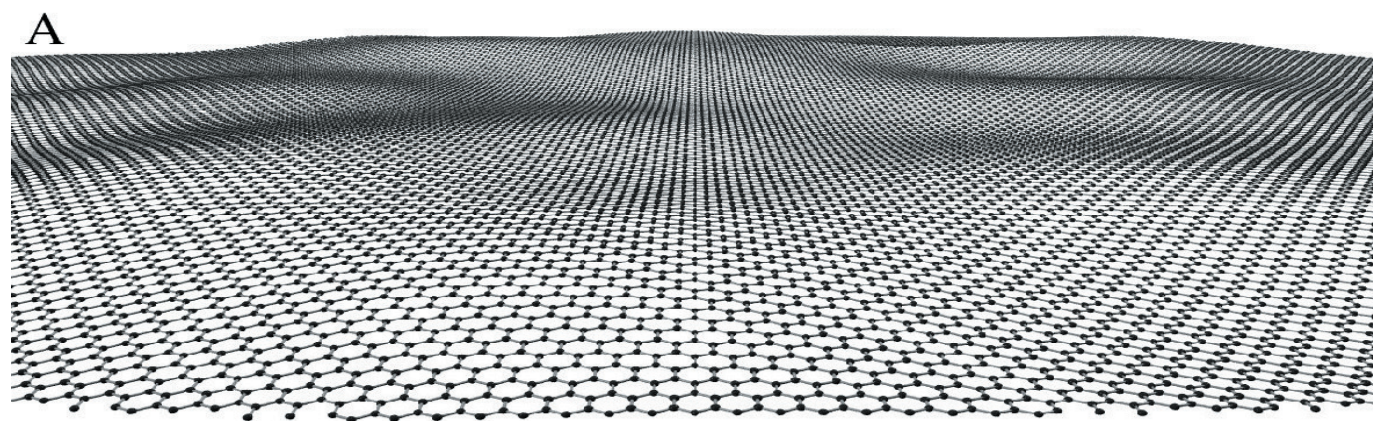
Figure S2: Modelling of crumpled graphene. Starting from a flat sheet (A), a number of random waves such as the one shown in B are introduced to form the randomly curved membrane (C).



B



Figure S3: A, Graphene sheet with ripples of, typically, 0.2 nm in height h and 2 nm in lateral size L . B, Simulated diffraction pattern. Such ripples are too small to explain our observations.



B



Figure S4: Stronger crumpling. A, Ripples are 0.5 nm in height and their typical size is 5 nm laterally. Ratio L/h is the same as in Fig. S3. B, Calculated diffraction patterns agree well with our experimental data.

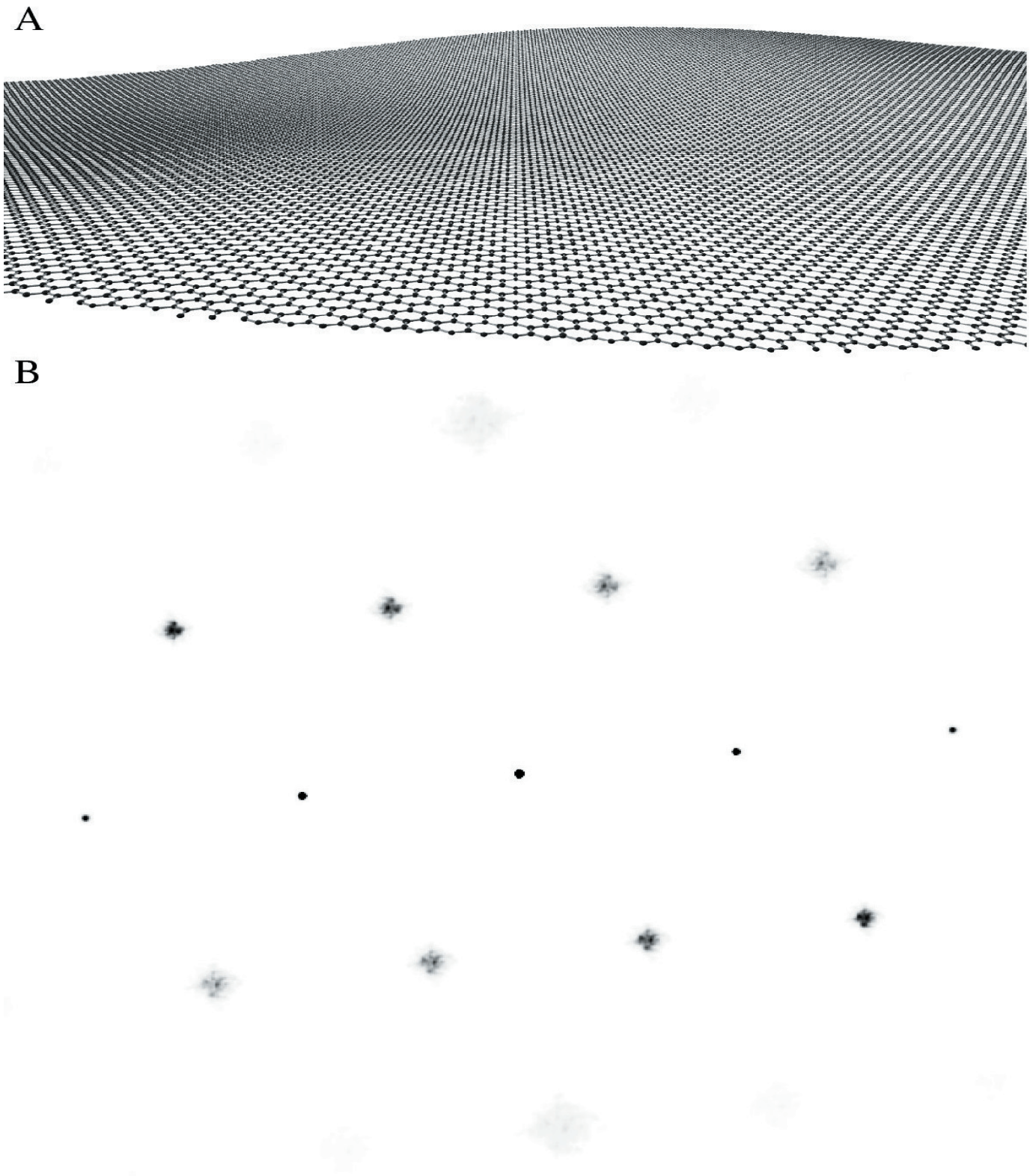


Figure S5: Ripples 2 nm high and 20 nm wide (A). Such large-scale crumpling leads to a non-Gaussian intensity distribution in the broadened diffraction peaks (B) which start reflecting specific distortions of a graphene sheet within the 250 nm diameter diffracting beam. Ripples of this size cannot be dominant in our membranes.